

DELFT UNIVERSITY OF TECHNOLOGY

BME MSc-THESIS

BM 51035

**Validation of a weight
compensation model for
wearable upper extremity
support system**

Authors: Zhangyue Wei

Student number: 5068142

Supervisor: Jaap Harlaar, Suzanne Filius

May 24, 2023



Abstract

DMD (Duchenne muscular dystrophy) is a genetic disorder characterized by progressive muscle weakness, leading to the eventual loss of muscle function. After losing lower extremity function, DMD patients lose the ability to use their arms. To assist individuals with DMD, an upper extremity exoskeleton is being developed to provide support.

The device is required to provide proper weight compensation for the weight of both the user and the support system. Previous literature review has highlighted three strategies for achieving compensation: Model, Calibration dynamic and Calibration static. However, the review lacks a conclusive understanding of the differences between these strategies. Thus, this study aims to validate a weight compensation model by comparing the joint torque with two different measurements: Calibration static and Calibration dynamic on non-disabled participants with a one DOF (Degree of freedom) elbow support system.

The weight compensation model was designed to accurately account for the weight of the user's arms and the exoskeleton device itself. It incorporates multiple inputs, including shoulder flexion, shoulder abduction, elbow joint angle, arm mass, and arm center of mass to calculate the required compensation torque for the motor located at the elbow joint.

The model was validated by a dead weight experiment. The weight compensation model was validated by comparing the joint torque measurements from Calibration dynamic and Calibration static results. Afterwards, experiments were performed on 12 male non-disabled participants. The weight compensation model results does not align well with the measurements from non-disabled participants. Analysis suggests that joint impedance caused these discrepancies. However, even after accounting for joint impedance, the weight compensation model still exhibits a tendency to overestimate the required compensation torque. A fitted model was used to decrease the product value of mass and center of mass to decrease overestimation. Furthermore, the comparative analysis indicates that dynamic and static measurements yielded similar mean values for joint torque.

While the weight compensation model demonstrates accuracy in a dead weight experiment under the assumption of an accurate estimation of its mass and center of mass, its performance is sub-optimal during the human experiment. This is attributed to the absence of joint impedance consideration and the overestimation of the forearm plus hand mass and center of mass for the user. Comparison between dynamic and static measurements the mean difference between dynamic and static measurements obtained from non-disabled participants indicates no substantial disparity in terms of joint torque.

Future plans for this research involve expanding the current one DOF configuration to a four DOF configuration and incorporating an inertial measurement unit (IMU) for more accurate angle measurements. Additionally, different compensation strategies will be compared in terms of task performance using metrics such as external interaction force or sEMG (surface electromyography). Lastly, the overestimation of forearm plus hand mass and center of mass will be further investigated.

Acknowledgments

I would like to express my heartfelt gratitude and appreciation to my supervisor Professor Jaap Harlaar and Suzanne Filius, for their invaluable guidance and support throughout my master's program. Their feedback and insight helped me to complete this research and write this thesis. I'd like also like to thank the external committee member Professor Frank Gijsen for spending time reading my thesis.

In addition, I'd like to appreciate my teammate Kyriacos Papa and other CBL group members, as they give value supports for this thesis.

Moreover, I would also like to thank my friends and family for their love and support during this process. Without them, this journey would not have been possible.

Finally, I would like to thank all of the participants in my study for their time. This work would not have been possible without their contribution.

Contents

1	Introduction	1
1.1	DMD	1
1.2	Literature review	2
1.3	Research Question	2
2	Compensation strategy	3
2.1	Model	3
2.2	Calibration dynamic	5
2.3	Calibration static	5
3	Dead weight experiment	7
3.1	Method	7
3.1.1	Dead weight configuration	7
3.1.2	Measure protocol	7
3.1.3	Data processing	8
3.2	Result	8
3.2.1	Model result vs Dead weight experiment measurement	8
3.2.2	Fitted model vs Dead weight experiment measurement	11
3.2.3	Dead weight measurement Calibration dynamic vs Cal- ibration static	14
3.3	Interpretation	14
4	Human experiment	17
4.1	Method	17
4.1.1	Initial measurement and parameter estimation	17
4.1.2	Human configuration	17
4.1.3	Measure protocol	19
4.1.4	Data processing	19
4.1.5	Outlier exclusion	20
4.2	Result	20
4.2.1	Model result vs Human experiment measurement	20

CONTENTS

4.2.2	Effect of joint impedance in Human experiment measurement data	20
4.2.3	Fitted model vs Human experiment measurement	24
4.2.4	Calibration dynamic measurement vs Calibration static measurement	27
5	Discussion	29
5.1	Dead weight experiment	29
5.2	Human experiment	30
5.2.1	Model vs Human experiment measurement	30
5.2.2	Fitted model vs Human experiment measurement	31
5.2.3	Human experiment Calibration dynamic measurement vs Calibration static measurement	32
6	Conclusion & Future work	33
6.1	Conclusion	33
6.2	Future work	34
7	Appendix	35
7.1	Dead weight data processing	35
7.1.1	Torque calculation	35
7.1.2	Data selection	38
7.1.3	Flexion Extension identification	40
7.1.4	Interpolation and averaging	40
7.1.5	Stats calculation	42
7.2	Initial measurement and Parameter estimation of the human experiment	42
7.2.1	Initial measurement	42
7.2.2	Mass estimation	43
7.2.3	Center of mass estimation	43
7.3	Human data process	43
7.3.1	Data exclusion	45
7.4	Data exclusion on Subject 03 and Subject 10	45

Chapter 1

Introduction

1.1 DMD

DMD (Duchenne muscular dystrophy) is a heritable genetic disorder affects mainly males (Bushby et al., 2010a). It is a X-linked disorder which leads to deletion of dystrophy gene (DMD;Locus Xp21.2). Biopsy results have shown that clusters of regenerated fibers with fibrosis and fatty infiltration in the muscle fibers (Mercuri et al., 2019). DMD Patients are unable to maintain contraction due to fiber degeneration (Angelini and Tasca, 2012).

Life expectancy of DMD patients have increased in recent years (Ellis et al., 2013), thanks to improvements in healthcare and related technologies like tracheotomy (Landfeldt et al., 2015). However, this also means DMD patients live longer time with arm disability and unable to perform routine task independently. Moreover, DMD patients were found to use more muscle capacity than healthy subject, leading to more frequent fatigue (Janssen et al., 2017). This highlights the emerging importance of providing proper support for DMD patients.

Upper extremities device provides weight compensation for both the user's arm and the device. After compensation, it eliminates the need for users to contract for weight compensation. It can be achieved by using a passive support, it uses spring or elastic band for compensation, has been used in DMD patients (Arakelian, 2015; Estilow et al., 2014). However in the late stage of DMD, patients are insufficient to maintain proper muscle contraction (Kumar and Phillips, 2013; Rahman et al., 2001). This means passive compensation is not enough to provide proper support. Therefore, an active compensation which has external power (Arakelian, 2015) is useful for late stage DMD users (Lobo-Prat et al., 2014).

The project (Wearable robotics project 7) aims to develop a wearable 4

DOF upper extremities support for DMD patients.

1.2 Literature review

A literature review was conducted to investigate implementation of weight compensation on upper extremities dynamic support device, which provides active support for users with upper extremities disabilities had been conducted. Three weight compensation strategies were identified: Model, Calibration dynamic and Calibration static.

The Model uses a mathematical model to estimate compensation. Most studies were found to use Lagrange model. In addition, most studies consider user's arm and device as an integrated object which shares a common mass and center of mass. The mass and center of mass of the body segment is estimated based on biometric table approximation, determined by ratio of body weight and arm length (Winter, 2009).

Calibration dynamic and Calibration static use the sample principle by utilizing pre-measured data to map system behavior (Lobo-Prat et al., 2016a). This approach requires two steps: First, the measurement phase records the relation between two variables like torque and angle position. Afterwards, in the execution phase, the measured data is used to perform task execution (McPherson et al., 2020). The difference between these two approaches is that during the measurement phase, the former measures the entire range of motion at low velocity (Lobo-Prat et al., 2016b, 2014), while the latter measures from several static postures (Just et al., 2020; Kooren et al., 2016).

The review concludes that it is not clear to find the best compensation strategy for the device among the three approaches. Thus, an experiment should be conducted to compare the differences between these strategies on non-disabled participants experimentally.

1.3 Research Question

This study aims to validate a weight compensation model by comparing the joint torque measurements using two different methods: Calibration dynamic and Calibration static, in non-disabled participants using a one DOF elbow support system.

Chapter 2

Compensation strategy

2.1 Model

The majority of studies in literature used mathematical model to estimate torque required for compensation. The most cited equations was the Lagrange equation (Spong et al., 2006) or Newton-Euler formula (He et al., 2005):

$$\tau = D(q)\ddot{q} + C(q, \dot{q})\dot{q} + g(q)$$

q represents the angular position of each joint, \dot{q} is the angular velocity and \ddot{q} represents the angular acceleration. $D(q)$ represents the inertia component and $C(q, \dot{q})$ represents the centrifugal term. $g(q)$ is the gravitational force and τ is the resultant net force or torque required to balance the gravitational and dynamics effect of the system (Liu et al., 2009; Rosen et al., 2005).

We made several assumptions to simplify modeling of the system: Firstly, friction between motors since a disturbance observer was available to compensate for friction internally. Secondly, the user's arm and the elbow support system were considered as two rigid links connected by a revolving joint at the elbow. Thirdly, a series elastic actuator was assumed to minimize effect of acceleration term and centrifugal terms (Oliveira et al., 2019). Additionally, since the system operated at a low velocity of 0.05rad/s, the influence of these terms were negligible. Therefore, only the gravity term was in the model:

$$\begin{aligned}\tau &= M * X * g * \sin(\beta + \theta) * \cos(\alpha) \\ M &= M_{arm} + M_{device} \\ X &= \frac{M_{arm} * X_{arm} + M_{device} * X_{device}}{M}\end{aligned}$$

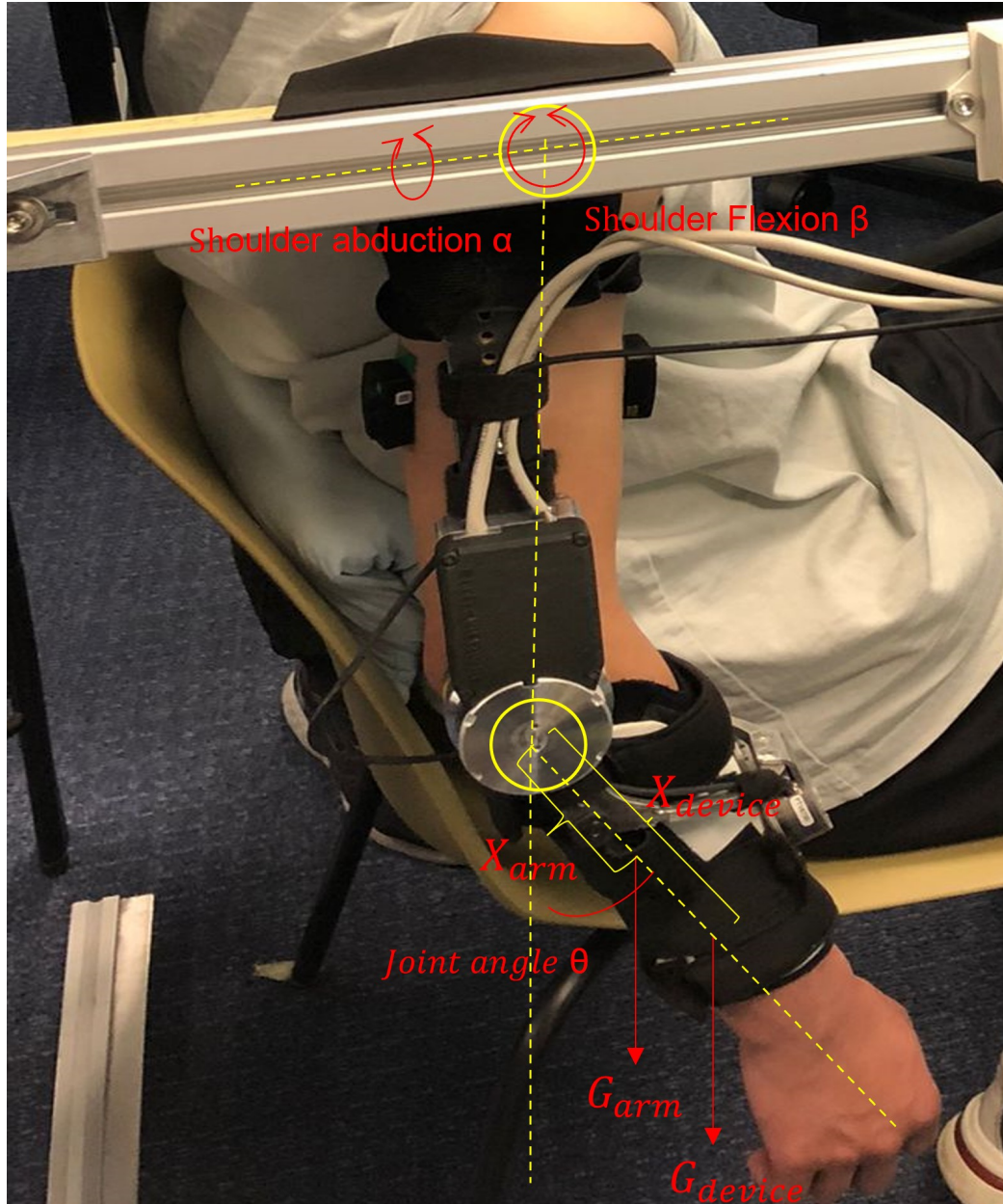


Figure 2.1: The model output is contingent upon several factors, this include mass and center of mass of the forearm plus hand; Mass and center of mass of the support system; Joint angle; Shoulder abduction and shoulder flexion.

CHAPTER 2. COMPENSATION STRATEGY

The M is the combined weight of the arm and the support system and X is the shared center of mass between user arm and the support system. β is the elbow flexion/extension, α is the shoulder abduction and θ is the joint angle (Figure 2.1).

The mass and center of mass of the forearm plus hand were estimated based on methods in literature (Winter, 2009). The support system center of mass was approximated by finding the balance point of each individual segment, while the mass of the support system was measured by disassembling it and measuring each part of the segment separately. Details can be seen in Appendix.

2.2 Calibration dynamic

To perform calibration dynamic measurement, the system moves at low velocity over the full range of motion. In our experiment, we designed the system to move at a constant low velocity within a defined range of motion with several repetitions. Details of the code can be seen at Appendix.

2.3 Calibration static

Calibration static measurement, the system were taken by moving between several static postures. In our experiment, the measurements were obtained while the system was moving between several stationary positions. This part of the code was created by my partner Kynricaos Papa and can be seen at Appendix.

CHAPTER 2. COMPENSATION STRATEGY

Chapter 3

Dead weight experiment

Before conducting experiments on non-disabled participants, the weight compensation model were validated by comparing it with the measured data from an external dead weight that was attached to the support system. The dead weight mass and center of mass were accurately measured, providing an accurate input to the model, thereby validating the weight compensation model.

3.1 Method

3.1.1 Dead weight configuration

In the dead weight experiment, a mass holder was used exclusively to this experiment. It securely hold the external weight attached to the support system (Fig 3.1).

3.1.2 Measure protocol

A 1kg dead weight was attached to the support system at a distance of 0.138m from the elbow rotating center. Measurements were taken using both the Calibration static and Calibration dynamic methods. A diagram is shown in (Fig 3.2).

For Calibration dynamics, the abduction angle was set at 0 deg. It moved at a constant velocity (0.05 rad/s) within the lower bound and upper bounds with 10 repetitions.

For Calibration statics, the abduction angle was also set at 0 degree. The system moved and paused at each designated static position interval for measurement. A total of 24 intervals were recorded.

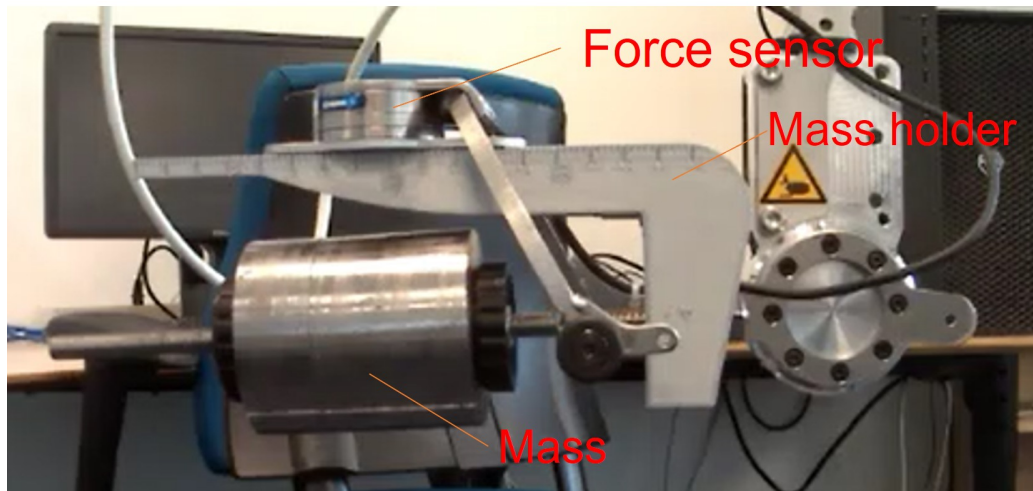


Figure 3.1: The mass holder with 1kg dead weight attached at 0.138cm mark. It was installed beneath the force sensor and consisted of a plastic structure with a length mark for accurate measurement. A metal bolt was inserted beneath the plastic structure to support the attached dead weight.

3.1.3 Data processing

The force data obtained from force sensors underwent several processing steps with included filtering, rotation and transformation of the data into elbow joint torque. After calculating the joint torque, the RMS (root-mean-square) and coefficient of determination were computed to assess the model's output against the measured result. Details about data processing can be seen in [Appendix: Dead weight data processing](#).

3.2 Result

3.2.1 Model result vs Dead weight experiment measurement

The Result indicates that the difference between measurements and the model results is small as shown in [Fig 3.3](#), [Fig 3.4](#) and [Table 3.1](#): The average difference is less than 0.1 Nm with a high coefficient determination. However, there are some discrepancies: The model is different to the measurement result at high and low joint angle. In addition, the maximum peak of the measured result is shifted to the right by 5.92 deg for dynamic measurement and 5.11 deg for static measurement while it was expected to be located at

CHAPTER 3. DEAD WEIGHT EXPERIMENT

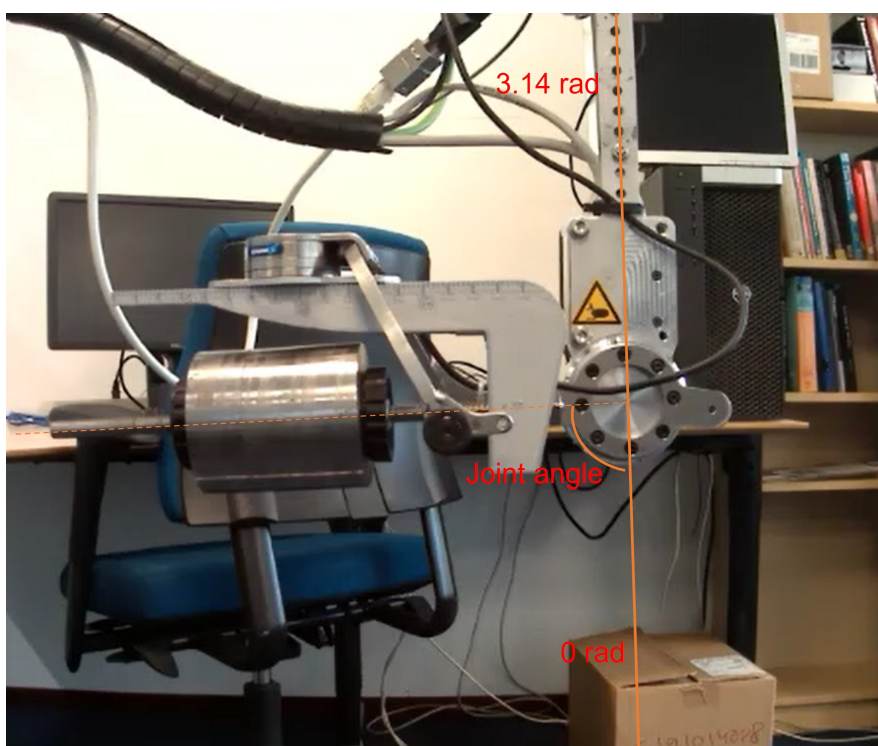


Figure 3.2: The system moved between lower and upper bound, Calibration dynamic moves at constant velocity while Calibration static moves between several static positions.

CHAPTER 3. DEAD WEIGHT EXPERIMENT

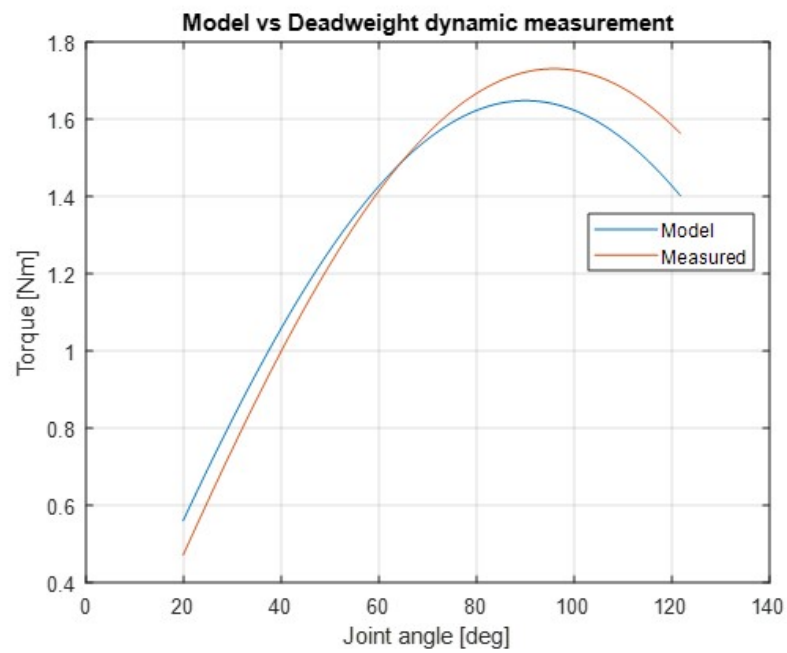


Figure 3.3: The plot contains result of two curves: The blue line represents the model result and the red one represents the measured dynamic result.

CHAPTER 3. DEAD WEIGHT EXPERIMENT

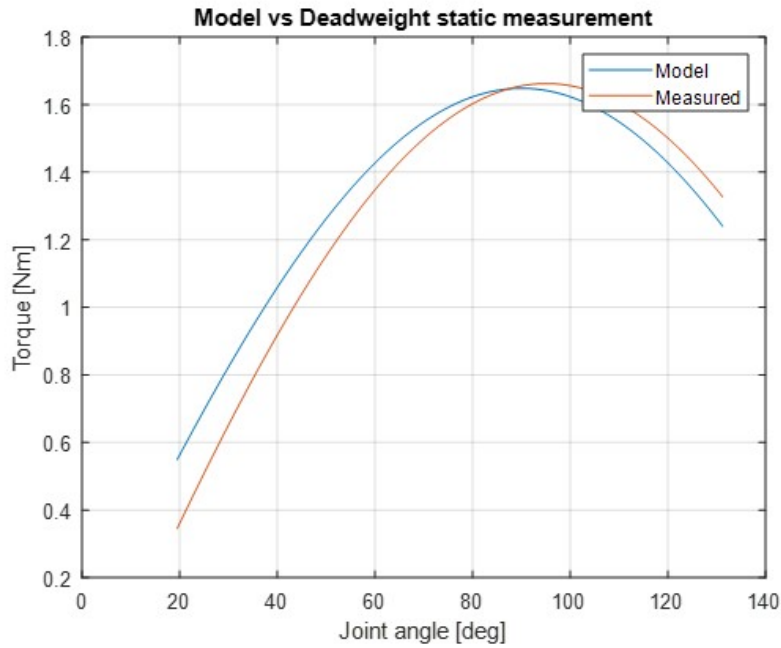


Figure 3.4: The plot contains result of two curves: The blue line is the model result; The red one is the measured static result.

90 deg.

Type	Comparison	RMS (Nm)	R^2
Dynamic	Model vs dead weight measurement	0.0810	0.953
Static	Model vs dead weight measurement	0.0975	0.931

Table 3.1: This table presents the value of root means square error and coefficient of determination between model output and measured result from the dead weight experiment.

3.2.2 Fitted model vs Dead weight experiment measurement

In Fig 3.3 and Fig 3.4, result indicates that the measurements have peak shift and the value between the measured data and the model output is different. To address this, a fitted model was used to shift the model to match the maximum peak and adjusted the product value of the dead weight's mass

CHAPTER 3. DEAD WEIGHT EXPERIMENT

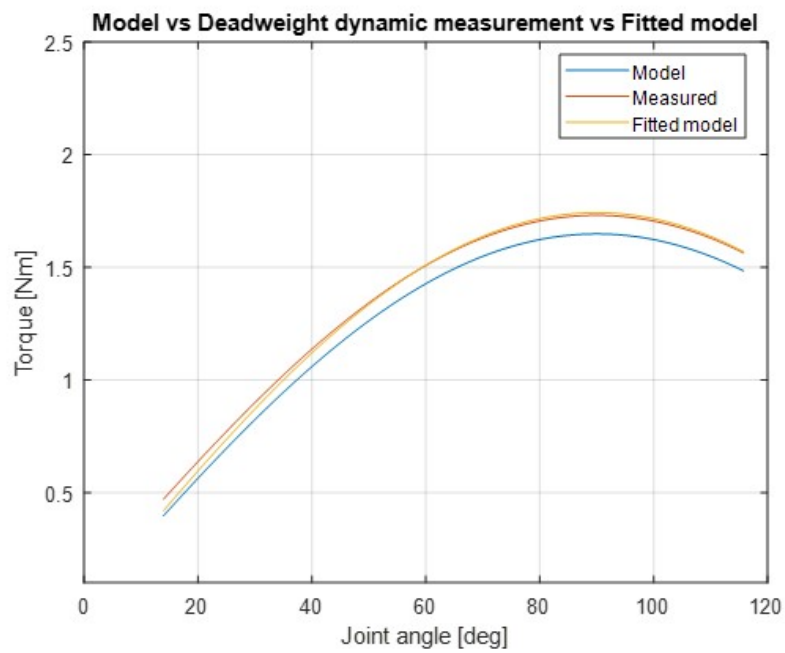


Figure 3.5: The plot contains result of three curves: The blue line represents the model result after shifting its maximum to the measured result, the red one represents the measured dynamic result and the orange line represents the fitted model which not only shifts the maximum but also adjusts the product value of the dead weight's mass and center of mass to fit to the measured result.

CHAPTER 3. DEAD WEIGHT EXPERIMENT

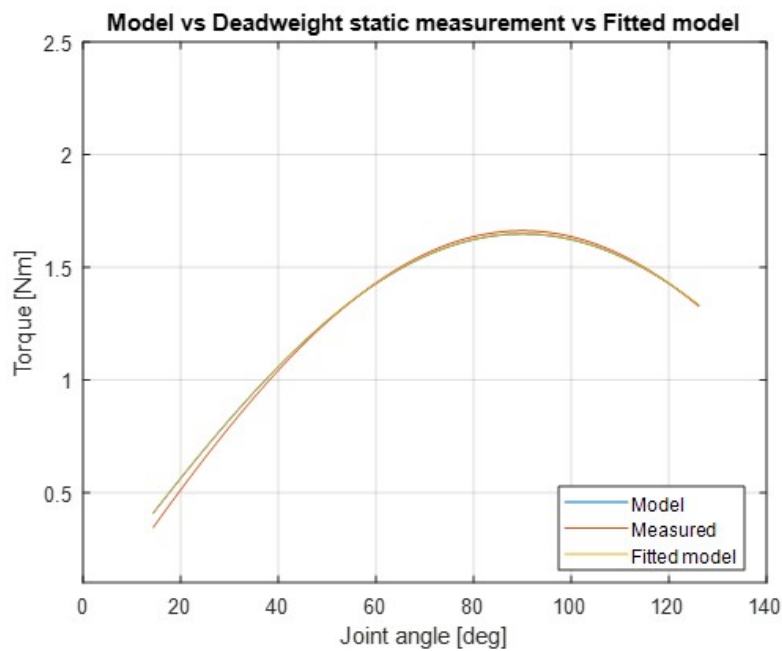


Figure 3.6: The plot contains result of three curves: The blue line is the model result after shifting its maximum ; The red line is the measured static result. The orange line is the fitted model which shifts the maximum and fits to the measured result and it is overlapped with the model curve.

CHAPTER 3. DEAD WEIGHT EXPERIMENT

and center of mass so that the fitted model is aligned with the measurements:

$$\min_a error = \sqrt{\frac{\sum_{n=1}^n (T_{model_n} - T_{measure_n})^2}{n}}$$

The T_{model} is the estimated value from model based on parameter, $T_{measure}$ is the interpolated measure data with n samples so that the sample size between measured data and model is matched to calculate mean error, while "a" is the product value of mass and center of mass. The cost function used Matlab function "fmincon" to optimize by changing the product value of the forearm plus hand's mass and center of mass.

After shifting and fitting, the resulting plot shows a better alignments, as seen in Fig 3.5 and Fig 3.6. Furthermore, the RMS is reduced by a factor of eight time lower and the coefficient of determination also increases compared to the original result (Table 3.2).

Type	Comparison	RMS (Nm)	R^2
Dynamic	Model vs dead weight measurement	0.0190	0.997
Static	Model vs dead weight measurement	0.0212	0.997

Table 3.2: This table presents the value of root means square error and coefficient of determination between the fitted model output and measured result from the dead weight experiment.

3.2.3 Dead weight measurement Calibration dynamic vs Calibration static

Result shows that the difference between Calibration dynamic and Calibration static is small, the averaged torque difference between two measurements are 0.078Nm (Fig 3.7).

3.3 Interpretation

In this dead weight experiment, a dead weight with known mass and center of mass was attached to the support system. The measurements were performed based on the principles of Calibration dynamic and Calibration static measurement. Measured results were compared with output of the weight compensation model.

The comparison between the model and two measurements shows a low RMS with a high coefficient of determination. Therefore, it can be concluded

CHAPTER 3. DEAD WEIGHT EXPERIMENT

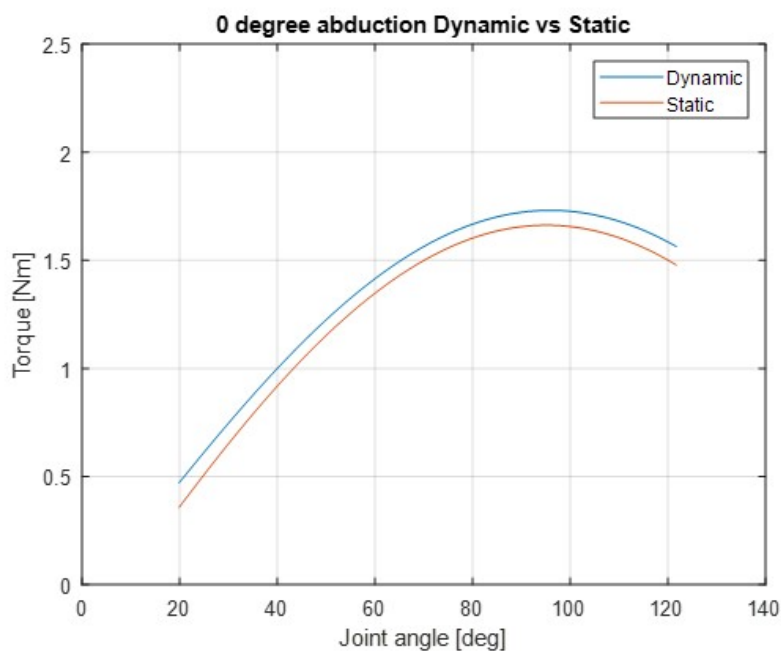


Figure 3.7: The plot contains result of two curves: The blue line represents the Calibration dynamic result and the red line is the Calibration static result. The static result is re-interpolated to the same joint angle as the dynamic measurement.

CHAPTER 3. DEAD WEIGHT EXPERIMENT

that under dead weight condition, assuming there is an accurate measurement of input parameters, the model was validated.

Chapter 4

Human experiment

After validating the model in the dead weight experiment. The weight compensation model was compared with the measured result from non-disabled participants.

4.1 Method

4.1.1 Initial measurement and parameter estimation

On Aug 2022, 12 male participants volunteered to participate in the experiment. Each participant had signed the consent and this experiment was approved by the Human research Ethics Committee (HREC).

Prior to the experiment, various initial measurements were taken for each participant, including their body weight, body height and arm length. Water displacement method was used to measure arm and hand's volume. Following the protocol described by Winter(2009), the mass and center of mass of the forearm plus hand were estimated based on previous measurements (Winter, 2009). Details about parameter approximation is available in [Appendix: Initial measurement and Parameter estimation of the human experiment](#).

4.1.2 Human configuration

An arm cuff was designed to fit the participant's right forearm was installed on the system. To ensure the participant's comfort, filling material was added to the cuff and its weight was taken into account in the weight compensation model. Furthermore, two EMG sensors were attached to participant's right forearm, one at the tricep and the other one at the bicep ([Fig 4.1](#)).

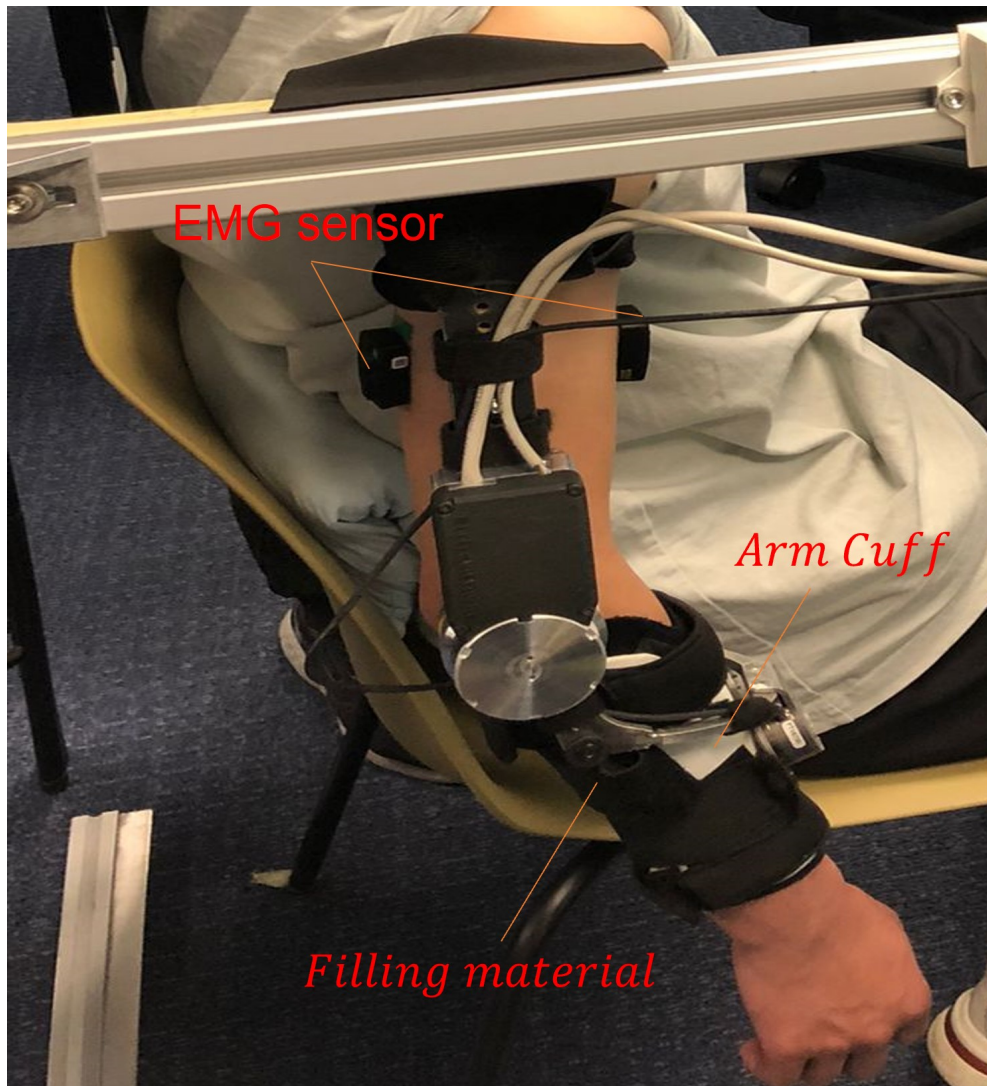


Figure 4.1: Participant's right arm attached to the elbow support system.

4.1.3 Measure protocol

The participant was strapped onto the system and was asked to move its arm to the maximum extension and flexion position within its comfort range and these two angle positions were recorded. The measurable range was determined by considering only 80% of the range in between these two angles.

After determining the measurable range of the participant, two measurement sessions were taken: one for Calibration dynamic and one for Calibration static. Both measurements were taken at 15 deg abduction angle, this was different from the dead weight experiment since during pilot experiment we observed that at 0 deg abduction, the participant's arm was impeded by its leg, thereby effecting measurement values.

Furthermore, the calibration matrix was different for each participant. As a result, each measurement had an individual calibration trial. Before each measure attempt, a position signal was sent to the system, it kept the joint angle at 90 deg position and measured the calibration data for the measurement.

In dynamics, a calibration measurement was taken to obtain calibration matrix for the force sensor. The system kept the participant's arm at 90 deg position for 30 seconds. Then, starting from the lower bound, the system moved with the participant's arm at a constant velocity (0.1 rad/s) and returned to the lower bound from the upper bound position. This cycle was repeated for eight times.

In statics, a calibration measurement was taken to obtain the calibration matrix for the force sensor. The system kept the participant's arm at 90 deg position for 30 seconds. Then, the device moved and paused at each record interval position for 10 seconds. Each static measurement had 24 intervals.

During the measurements, a camera was used for recording. The face of the participant was blurred to protect its privacy. Simultaneously, data from EMG and force sensor was extracted, processed and saved. All data and experiment notes were saved in Elabjournal.

4.1.4 Data processing

After data was collected, further processing was required. Similar to the dead weight experiment, the process involved calculation of joint torque, as well as the averaging and calculation of RMS and coefficient of determination between the model and measured results.

Moreover, an additional exclusion procedure was implemented: First, the first and the last cycle were automatically excluded. Second, exclusion based on EMG to remove any cycles in which the participant's muscle activity

was deemed too high. Third, the exclusion based on video inspection if participant had behavior which effected force measurement. Details about human experiment data processing can be seen in [Appendix: Human data process](#).

4.1.5 Outlier exclusion

After data processing, each participant force data was plotted under the same scale for comparison. Result showed that the deviation of Subject 03 and Subject 10 was obvious to be outliers thus in the following result section does not exhibit result from Subject 03 and Subject 10. Detailed explanation can be seen in [Appendix: Data exclusion of Subject 03 and Subject 10](#).

4.2 Result

4.2.1 Model result vs Human experiment measurement

Type	Comparison	RMS (Nm)	R^2
Dynamic	Model vs Human measurement	0.757 ± 0.096	0.414 ± 0.192
Static	Model vs Human measurement	0.494 ± 0.209	0.692 ± 0.265

Table 4.1: This table presents the value of RMS and coefficient of determination between model output with measured joint torque result calculated from participant force data.

The results from the dynamic measurement in the human experiment showed a substantial difference between the model and the measurement from the participant. The averaged difference between the model and the dynamic measurement is illustrated in [Fig 4.2](#) and [Fig 4.3](#). At lower joint angles, the measured joint torque was lower than the model prediction and was below zero, while at higher joint angles, the measured joint torque was higher from the model prediction, this lead to a higher RMS and a lower coefficient of determination than those obtained from the measurement in dead weight experiment ([Table 4.1](#)).

4.2.2 Effect of joint impedance in Human experiment measurement data

One of the crucial factors that differ between difference between a measured joint torque from the dead weight and a participant is joint impedance. Dur-

CHAPTER 4. HUMAN EXPERIMENT

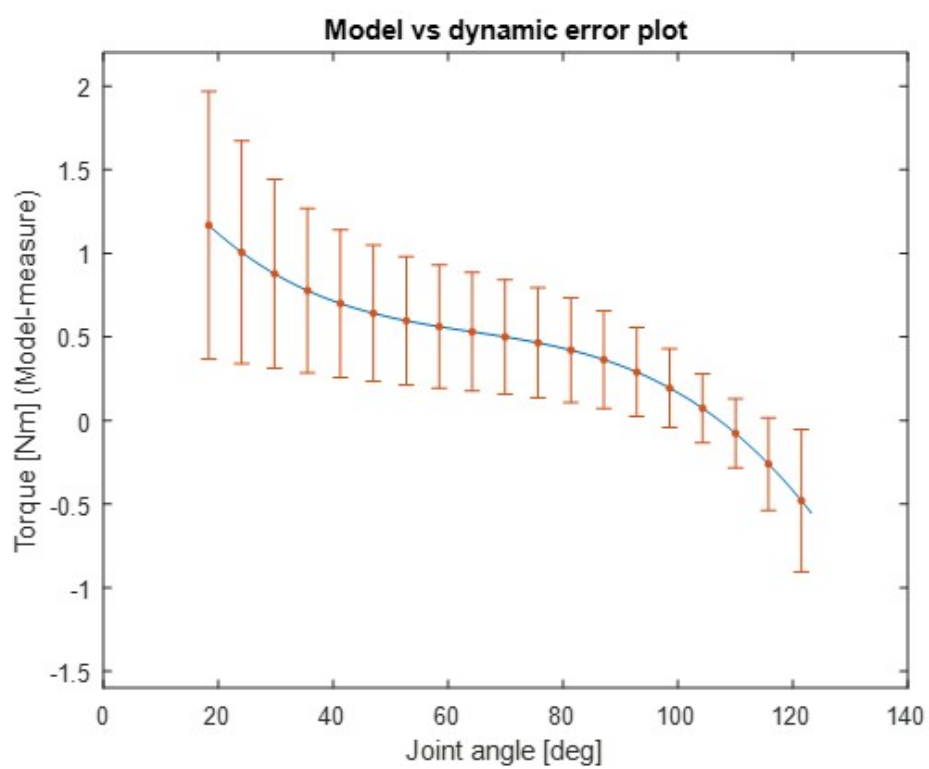


Figure 4.2: The plot exhibits the mean and standard deviation difference between the weight compensation model and the dynamic measurement vs the joint angle.

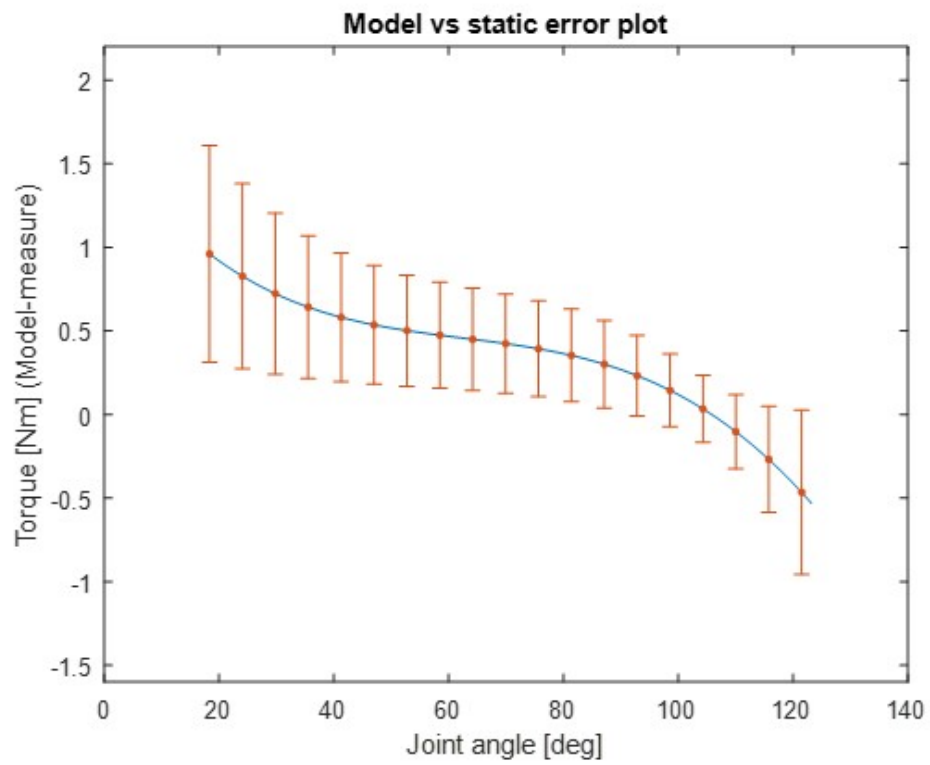


Figure 4.3: The plot exhibits the mean and standard deviation difference between the weight compensation model and the dynamic measurement vs the joint angle.

CHAPTER 4. HUMAN EXPERIMENT

ing the experiment, a measurement was taken at an abduction angle at 90 deg which was not mentioned during the as it was not directly relevant to the topic of gravity compensation since at 90deg abduction, the compensation plane was not affected by gravity. In our model, at 90 deg abduction angle, the output was zero regardless of other parameter values. Hence, this measurement showed how other forces like joint impedance beside gravity contributes to shaping of the measured torque curve.

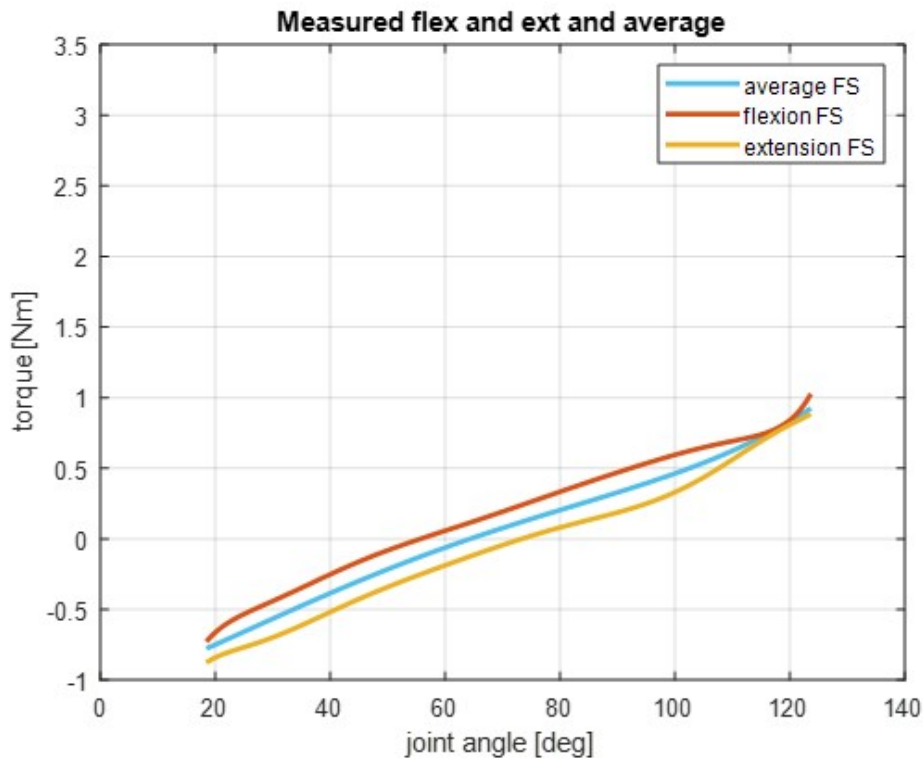


Figure 4.4: This plot shows the averaged result of joint impedance of Subject 01, calculated based on the averaged extension and flexion measurement while measured at 90 deg abduction angle.

The measurement of Subject 01 at 90 deg abduction had a value below zero at lower angles, as seen in Fig 4.4.

Assuming the subject has the same joint impedance while measuring at 90 deg and 15 deg abduction, the curve could be refit and re-interpolated from these two measurements to the same data size, making a subtraction possible. The effect of 90 deg abduction measurement subtraction is illustrated in Fig 4.5 for dynamic measurement and Fig 4.6 for static measurement. After subtraction, the model output is higher than the measurement, the difference

between model and the measurement peaks around 90 deg, then decreases at higher joint angle. Results of RMS and coefficient of determination is illustrated in Table 4.2. The RMS error did not substantially change after joint impedance subtraction. The coefficient of determination, on the other hand, was substantially higher.

Type	Comparison	RMS (Nm)	R^2
Dynamic	Model vs Human measurement	0.705 ± 0.340	-3.184 ± 2.277
Static	Model vs Human measurement	0.590 ± 0.346	-1.661 ± 1.860

Table 4.2: This table represents the value of RMS and coefficient of determination between model output and measure joint torque after joint impedance subtraction.

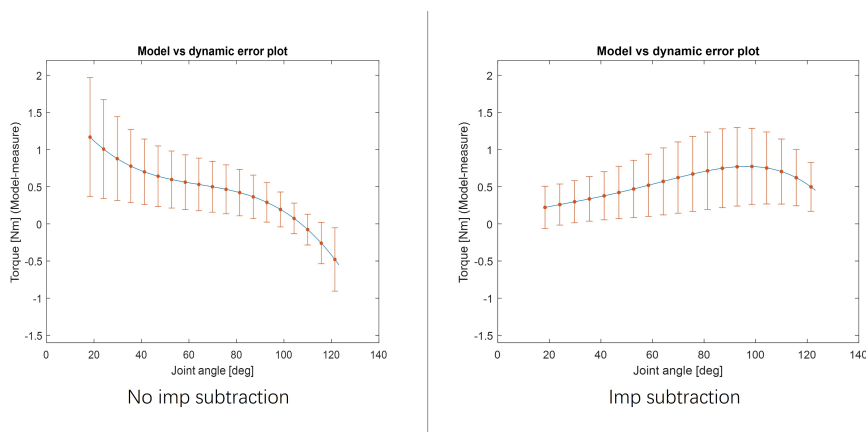


Figure 4.5: The plot presents the mean and standard deviation difference between a 15 deg dynamic measurement with 90 deg measurement subtraction (Right) or one without (Left).

4.2.3 Fitted model vs Human experiment measurement

In the dead weight experiment, the model was validated by assuming a correct approximation of the attached weight's mass and center of mass. However, in human experiment, it was found that the model substantially overestimated the joint torque even after accounting for joint impedance. This suggests that there is an overestimation of the participant's forearm plus hand mass and center of mass in the model.

CHAPTER 4. HUMAN EXPERIMENT

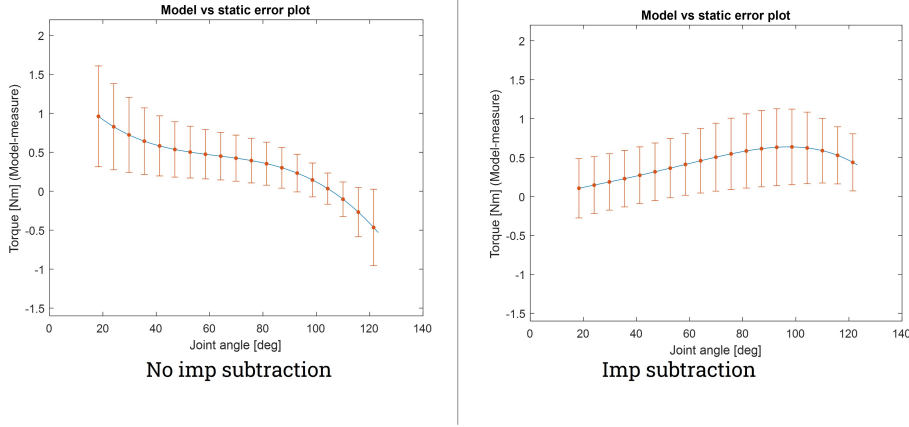


Figure 4.6: The plot presents the mean and standard deviation difference between a 15 deg static measurement with 90 deg measurement subtraction (Right) or one without (Left).

To address this issue, a fitted model was used to find the best match between model and the measured result by minimizing the error function:

$$\min_a error = \sqrt{\frac{\sum_{n=1}^n (T_{model_n} - T_{measure_n})^2}{n}}$$

The T_{model} is the estimated value from model based on parameter, $T_{measure}$ is the interpolated measure data with n samples so that the sample size between measured data and model is matched to calculate mean error, while "a" is the product value of mass and center of mass. The cost function used Matlab function "fmincon" to optimize by changing the product value of the forearm plus hand's mass and center of mass.

The effect of fitted model is illustrated in Fig 4.7 for dynamic and (Fig 4.8) for static correspondingly. The mean of the difference between fitted gravity model and measured result become much smaller after fitting the curve, especially between joint angles of 40 to 100 deg. However, the fitted model still exhibits high standard deviation of error at lower and high joint angle. Overall, result showed a decrease in RMS and a increase in coefficient of determination (Table 4.3). In addition, the fitted model decreased the original product value of mass and center of mass, thereby decreasing the overall value of joint torque output (Table 4.4).

CHAPTER 4. HUMAN EXPERIMENT

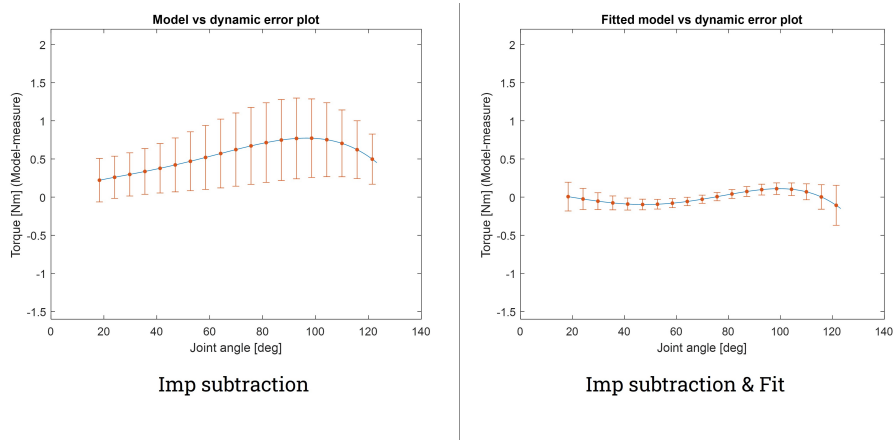


Figure 4.7: The plot presents the mean and standard deviation difference between a 15 deg dynamic measurement subtracts 90 deg measurement with fitted model (Right) and without (Left).

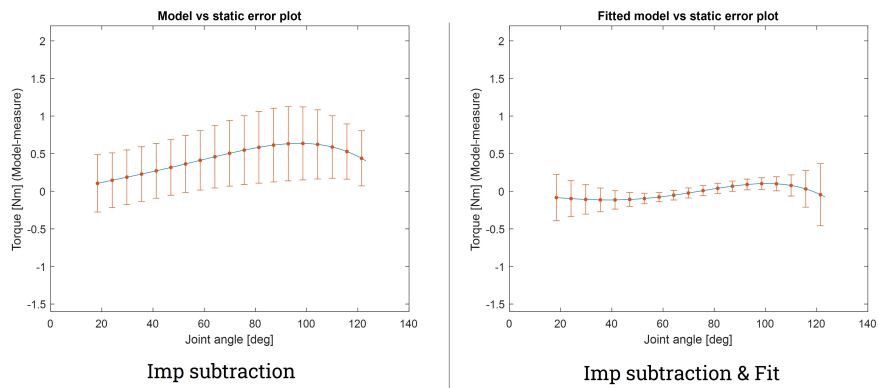


Figure 4.8: The plot presents the mean and standard deviation difference between a 15 deg static measurement subtracts 90 deg measurement with fitted model (Right) and without (Left).

Type	Comparison	RMS (Nm)	R^2
Dynamic	Fitted model vs Human measurement	0.111 ± 0.042	0.842 ± 0.228
Static	Fitted model vs Human measurement	0.142 ± 0.058	0.739 ± 0.301

Table 4.3: Group result of the fitted model vs Measured results with 90 deg joint impedance subtraction.

CHAPTER 4. HUMAN EXPERIMENT

Table of Mass*Center of Mass(kg*m) after joint impedance subtraction	
Change of parameter in dynamic	Change of parameter in static
0.084 ± 0.041	0.067 ± 0.045

Table 4.4: This table shows the fitted model decrease the product value of mass times center of mass. As a result, the fitted model has a lower joint torque than the model.

4.2.4 Calibration dynamic measurement vs Calibration static measurement

The measurement result of Calibration dynamic and Calibration static was compared for each participant, as illustrated in Fig 4.9.

Result shows that Calibration dynamic and Calibration static has similar mean and standard deviation distribution. This similarities also applies after joint impedance subtraction, the mean difference between dynamic and static 0.0832 ± 0.0063 Nm without joint impedance subtraction and 0.1141 ± 0.0496 Nm with joint impedance subtraction.

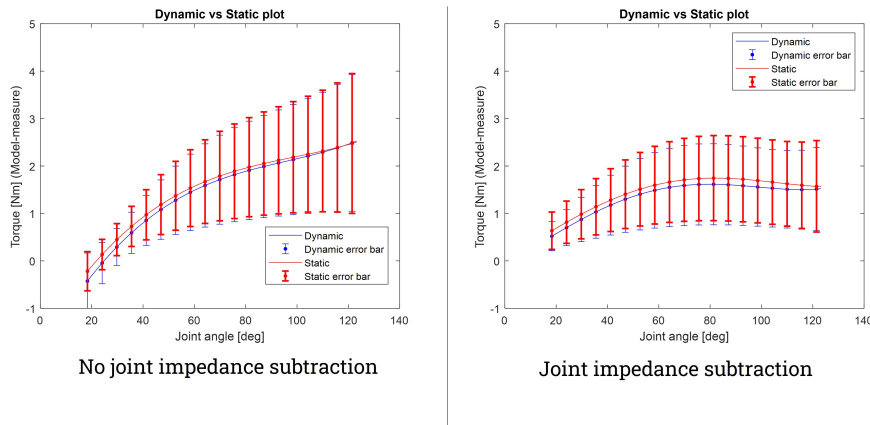


Figure 4.9: The plot presents the mean and standard deviation of measured Calibration dynamic and Calibration static result at 15 deg, with joint impedance subtraction (Right) and without (Left).

CHAPTER 4. HUMAN EXPERIMENT

Chapter 5

Discussion

5.1 Dead weight experiment

The result show that both the dynamic measurement and the static measurement have a low RMS (0.081 Nm for dynamic and 0.0975 Nm for static), relative to the overall range of measured torque which is 5% and a high coefficient of determination. This indicates that the model closely approximates the measured data and has a similar shape.

However, a slight 5 deg maximum peak shift to the right direction are observed in both measurement conditions which may be due to changes in the calibration matrix during the experiment. As the calibration was not performed immediately before the dead weight experiment, the rotation of the system might had slightly changed due to factors such as hardware re-assembling. The model was improved by using a fitted model to shift the model and adjusted the product value of the mass and the center of mass. This suggests that if the angle shift is resolved, the model could achieve better estimation. Therefore, it is essential to perform a calibration trial before measure experiment to ensure accuracy of the measurements.

Comparison between the dynamic and the static measurement exhibits an averaged of 0.078Nm difference in the 1kg dead weight condition, which is 4% of the overall range. This suggests that there are no substantial difference between the dynamic and static measurement.

Overall, the validation of the weight compensation model is successful and it demonstrates that the model can accurately the weight compensation at different joint angles, provided that the input parameters, such as the forearm plus hand's mass and center of mass are accurately measured.

5.2 Human experiment

5.2.1 Model vs Human experiment measurement

In contrast to the dead weight experiment, the results of the human experiment are different. The RMS increase ten-fold, relative to the overall range of measured torque is around 23% for dynamic and 20% for static. These values are much higher than those reported in a similar study (Xie et al., 2021). The coefficient of determination also substantially decreases comparing to the dead weight experiment, indicating that the model does not match the shape of the measurement. These values are also much lower than reported in the similar study Guidali et al. (2013). Furthermore, error plot (Fig 4.2) (Fig 4.3) shows that the difference between model and measurement are influenced not only by gravity, otherwise the plot should exhibit shape like a "bell" curve.

The discrepancies between the dead weight experiment and the human experiment may be attributed to factors such as inertia and joint impedance. Inertia could vary due to different of mass while joint impedance could be attributed to intrinsic properties of the joint, tissues, muscles and connective tissues (Kearney and Hunter, 1990). The effect of inertia is expected to be minimal due to low velocity (0.1 rad/s) and presence of a series elastic actuator (Oliveira et al., 2019). Joint impedance, on the other hand, is expected to have a greater impact on the measurements. Previous study suggested that at low bandwidth movements, the major components are gravity and joint impedance. However, it remains unclear whether joint impedance affects the overall measurement (Kooren et al., 2016).

After subtracting assumed joint impedance from the 90-deg measurement, comparison (Fig 4.5) (Fig 4.6) of error plot shows that the difference between model and the measurement exhibits like a "bell" curve after subtracting 90 deg measurement, which peaks around 90 deg. This result suggest that overall, the model overestimates the measurement after subtracting 90 deg measurement. The coefficient of determination was substantially worse than the joint impedance subtraction. This suggests that the method was used to subtract joint impedance has several flaws, including the fact that the 90 deg measurement and 15 deg measurements were taken at different time. In addition, the elongated metal bar that connected to the elbow had bent down due to non-disabled participant's arms weight was observed during the 90 deg measurement, resulting in the gravity component being present in the 90 deg measurement.

In the literature review, most of the studies that used a model did not consider joint impedance. Therefore, it was assumed the joint impedance

CHAPTER 5. DISCUSSION

was not an factor in the gravity measurements for non-disable participants, as they does not have any muscle fiber lesions like those found in patients with DMD (Bushby et al., 2010b). However, based on the experiment result, the effect of joint impedance had substantially impacted measured joint torque at 15 deg even from non-disabled participants.

Overall, these results suggest that joint impedance is an important component in the measurement, even for a non-disable participant. Therefore, using a weight compensation model alone is not sufficient to represent the overall dynamics of the forearm at low velocity.

5.2.2 Fitted model vs Human experiment measurement

After joint impedance subtraction, the model value still overestimated the measured values, suggesting an overestimation of parameters.

The fitted gravity model was observed to be more aligned to the measured results as illustrated in Fig 4.7 and Fig 4.8, the difference between the fitted model and the measurement substantially decrease, in addition, the standard deviation of the difference substantially decreases. However, the fitted model does exhibits increase on joint torque standard deviation at low and high end joint angle, where the system turned direction, this might causes a lot of variability.

Further analysis reveals a decrease in the product value of participant forearm plus hand's mass and center of mass, under condition at 15 deg abduction, when joint angle is at 90 deg where the maximum gravity effect is present, the average change of the model output is 0.798 Nm for dynamic and 0.634 Nm static, indicating the fitted model substantially decreases overestimation.

One factor of uncertainty in the mass estimation was the assumption of a constant density for all participants, despite variations in muscularity due to differences in sport intensity, sport type and diet. It is known that muscles have a higher density than fat, thus a more masculine participants tends to have higher forearm density. Therefore, the use of a literature value for density estimation may lead to errors in the model.

Similarly, the estimation of the center of mass based on literature review from biometric table estimation using segment length can also introduce errors, as the density estimation may not be accurate. Additionally, the estimation of center of mass can vary among different subjects and can change during movement (Winter, 2009).

Overall, the finding suggest that the bio metric approximation leads to

overestimation of joint torque, thus the current way to estimate mass and center of mass needs reconsideration. It is unclear whether mass or center of mass has a greater impact on the overestimation, and further investigation is needed.

5.2.3 Human experiment Calibration dynamic measurement vs Calibration static measurement

As illustrated in the left of Fig 4.9, dynamic and static measurements exhibit similar mean and standard deviation value. Comparison between original dynamic measurement and static measurement indicates that the mean difference is small. The difference value however is different from the dead weight experiment (Fig 3.7) as dynamic is higher than the value of static. This is opposite for the human experiment. Possible factor could be due to the calibration matrix used in the dead weight experiment and addition of joint impedance.

As illustrated in the right of Fig 4.9, dynamic and static measurements exhibits similar mean and standard deviation value. However, after joint impedance subtraction, the mean and standard deviation difference slightly increase. This indicates that the 90 deg subtraction leads to this differences. As discussed before, possible factor could be joint impedance change between measurement. Nevertheless, the mean difference is 5% relative to the overall range of the measured torque thus the value discrepancies after joint impedance subtraction is acceptable.

Chapter 6

Conclusion & Future work

6.1 Conclusion

In Chapter 1, we introduced various weight compensation strategies to compensate for the weight component of the user's upper extremities and one DOF elbow support system, including a weight compensation model, Calibration dynamic and Calibration static. We define the research question: This study aims to validate a weight compensation model by comparing the joint torque measurements using two different methods: Calibration dynamic and Calibration static, in non-disabled participants using a one DOF elbow support system.

In Chapter 2, we explain how each compensation strategy was implemented in our experiment.

In Chapter 3, we validate the model based on measured results by attaching an external dead weight with confirmation of its mass and center of mass. We demonstrate that the model could predict measured data with a correct estimation of input parameters.

In Chapter 4, we employ the same methodology as in Chapter 3 to evaluate the model's performance with 12 non-disabled participants. Unlike results in Chapter 3, the model exhibited poor match with the measured results. We attribute joint impedance and parameter overestimation lead to this discrepancies. We implemented a fitted model to address these issues.

In Chapter 5, we discussed that the result from the dead weight experiment validates the model. However, we observed a maximum peak shift, which could be attributed to calibration matrix issues. This could be fixed by using the fitted model to realign the maximum peak.

In addition, we concluded that two factors lead to the discrepancies between the model and the measurements:

- Joint impedance had a substantial effect on measurement, even for non-disabled participants.
- The product value of the participant's forearm plus hand's mass and center of mass approximation was overestimating.

6.2 Future work

For the future work on this topic, there are several areas for improvement:

- Expansion of the exoskeleton to cover the full upper extremities from a single arm by increasing the degrees of freedom to a 4 DOF setup and developing a corresponding gravity compensation model.
- Installation of IMU to determine shoulder abduction and elbow extension angle. This was originally planned but was abandoned due to issues with the data algorithm. Usage of IMU could provide more accurate measurements of abduction angle and solve the metal bar bending issue at the 90 deg measurement by determining the actual abduction angle at the elbow and thereby eliminating effect of gravity at the 90 deg measurement.
- The weight compensation model is not sufficient to represent the overall dynamics of the forearm. Thus, an accurate muscle model addition is required.
- Comparison of different compensation strategies by asking participants to perform task like position tracking, Metrics like external force and EMG activity could be used to compare and identify the best compensation strategy that is most suitable for users and DMD patients in the future.

Chapter 7

Appendix

7.1 Dead weight data processing

This section explains detailed procedure on how force data were processed, this include various steps: torque calculation, data selection, flexion extension identification, interpolating and averaging, stats calculation as illustrated in flow chart [Fig 7.1](#).

7.1.1 Torque calculation

In data output, the SEA torque was recorded as "data.Actuator_Joint_Torque_Nm", not any initial process is required.

For force sensor, the raw data were recorded in six analog channels in unit of counts, then transformed into units of volts:

$$Analog_volt = \frac{Analog_bitcount * Max_volt}{Bit_counts}$$

Analog_bitcount is $2^{16}/2$ due to 16 bits, it starts from -32768 to 32767, Max_volt is 10 V due to range is from -10 V to 10 V, this equation and note was taken from "fun_FScalibrationsimulinkblock.m".

To transform data from voltage to force and torque units, a working matrix documented in "FS_copymanual of DAQ FT manual calculations.xls" was used:

$$Forcatorque_Forcesensor = Workingmatrix * Analogout_volt$$

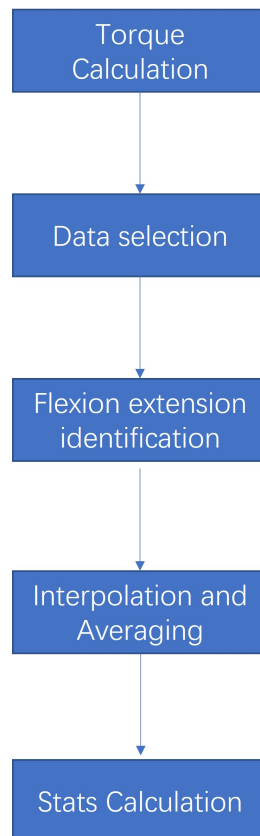


Figure 7.1: The work flow of processing joint torque subject data in the dead weight experiment.

CHAPTER 7. APPENDIX

Force sensor had bias in six directions: $F_x F_y F_z M_x M_y M_z$, in respect to the force sensor local coordinate, the value was measured in April by Kyriacos Papa. By subtracting the calibration matrix, the force sensor value was calibrated, assuming the value was consistent for all measurements:

$$Forcetorque_Forcesensor = Forcetorque_Forcesensor - Calibration_Matrix$$

The calibrated data was based on coordinate of the force sensor, which was located around the elongated superstructure of the exoskeleton, thus to get torque from the elbow motor, rotation and translation matrix was implemented to transfer to the elbow coordinate, as illustrated in Fig 7.2:

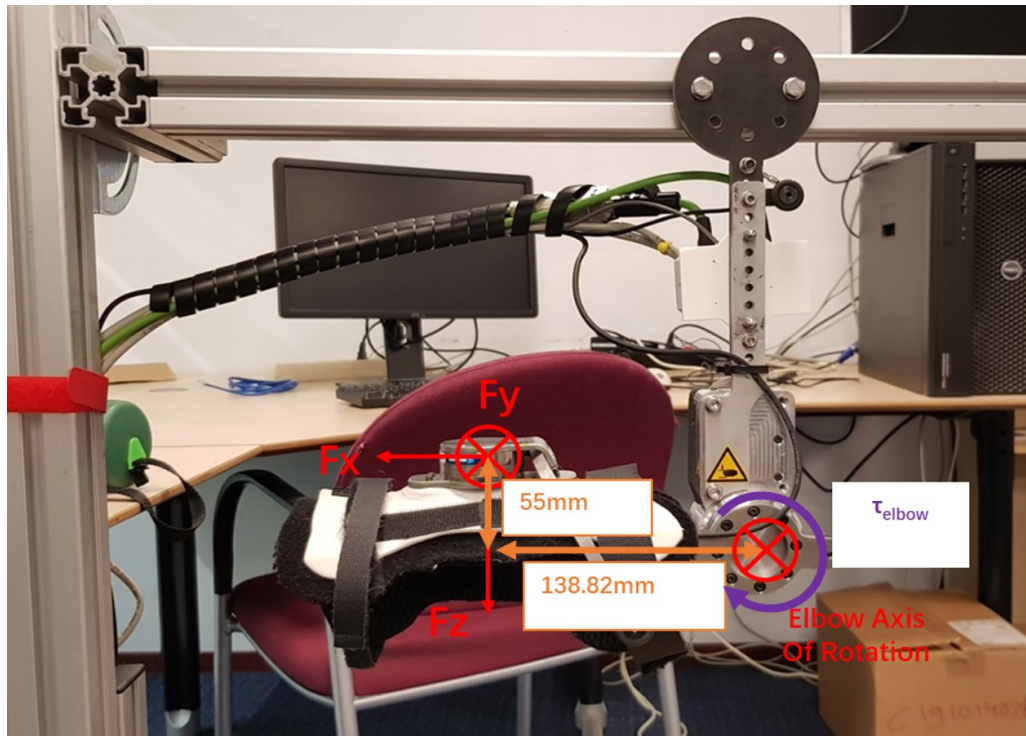


Figure 7.2: The coordinate starts from the force sensor and ends at the elbow joint.

$$Forcetorque_elbow = Transformation_matrix * Rotation_matrix * Forcetorque_Forcesensor$$

The final Force_torque_elbow is expected to have 6 strains of data which corresponds to $F_x F_y F_z M_x M_y M_z$ respectively, M_y is the elbow torque.

7.1.2 Data selection

First, a screen showing the object position over time will pop up, it ask users to define points, this helps system to recognize flexion and extension.

The dynamic measurement needs to define three points: Start of the cycle; First peak; End of the cycle (Fig 7.3). This part of code was in fun GetGinputInput.m created by Suzanne Filius.

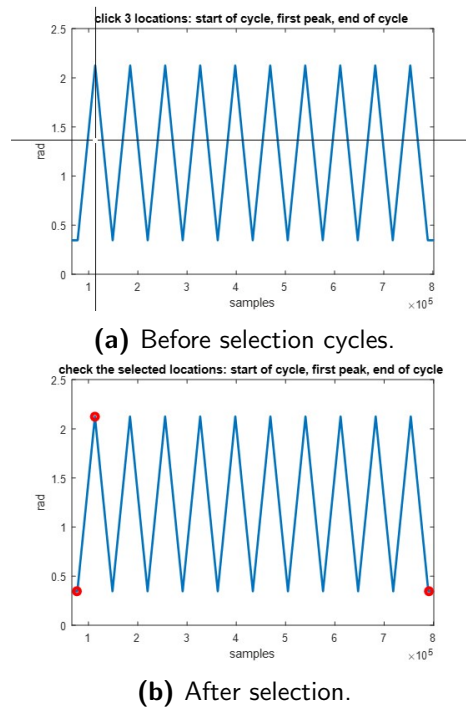
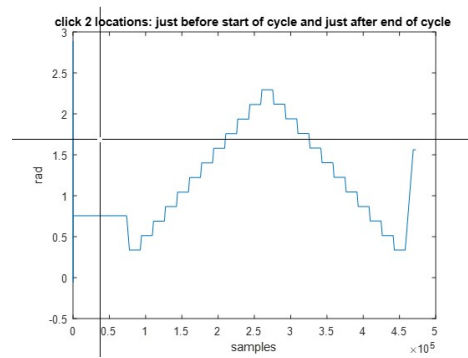


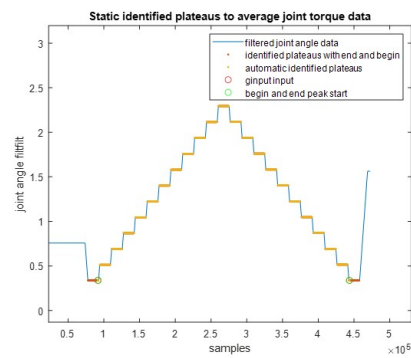
Figure 7.3: The plot is showing joint angle position vs samples. The users needs to select three locations: Start of cycle; First peak; End of the cycle. This helps the function identify flexion and extension peak.

The static measurement needs to define two points: Start of cycle; End of the cycle (Fig 7.4). This part of code was in fun GetGinputInput.m created by Suzanne Filius.

CHAPTER 7. APPENDIX



(a) Before selection cycles.



(b) After selection.

Figure 7.4: The plot is showing joint angle position vs samples. The users needs to select two locations: Start of cycle; End of the cycle. This helps the function identify flexion and extension peak.

7.1.3 Flexion Extension identification

Then, based on selection, the function will identify each flexion and extension movement in the cycle (Fig 7.5), each cycle data are collected, filtered and stored as struct array. This part of the code is achieved by function "make_flex_ext_struct" created by Suzanne Filius.

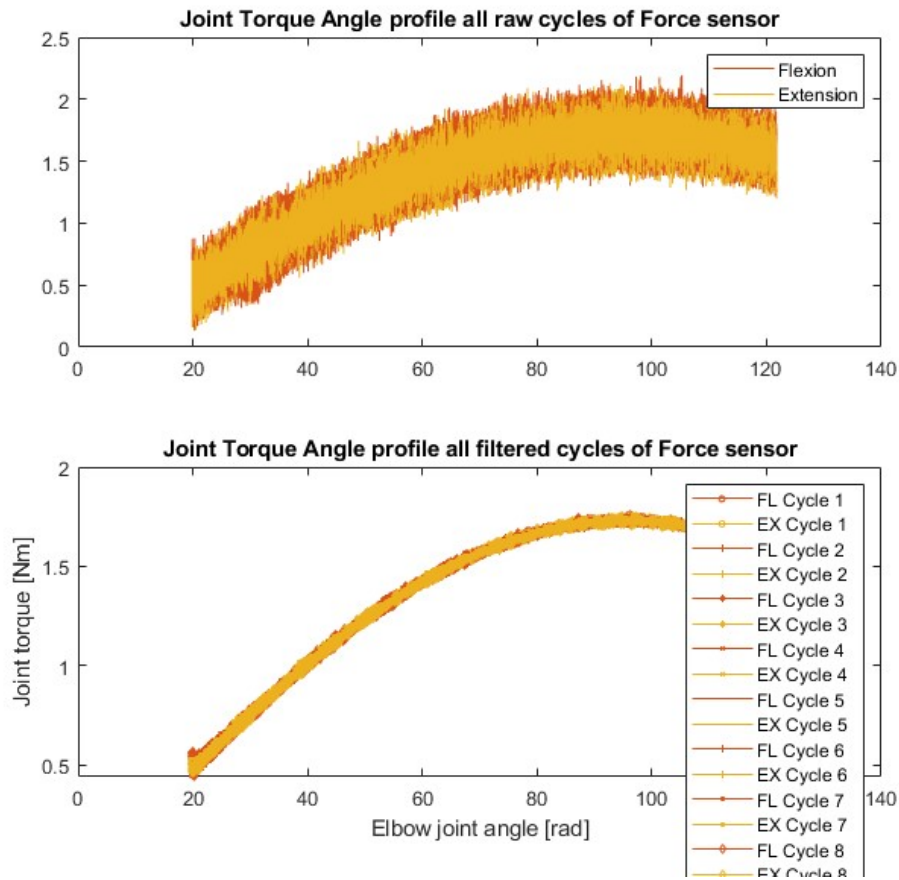


Figure 7.5: The function separate data based on number of cycles and flexion/extension directions

7.1.4 Interpolation and averaging

After obtaining filtered raw data from each cycle, an important process is interpolate each cycle from filtered data so that each cycle is down sampled to the same size, this makes averaging possible: By calculating averaged polyfit equation of flexion and extension curve (Fig 7.6).

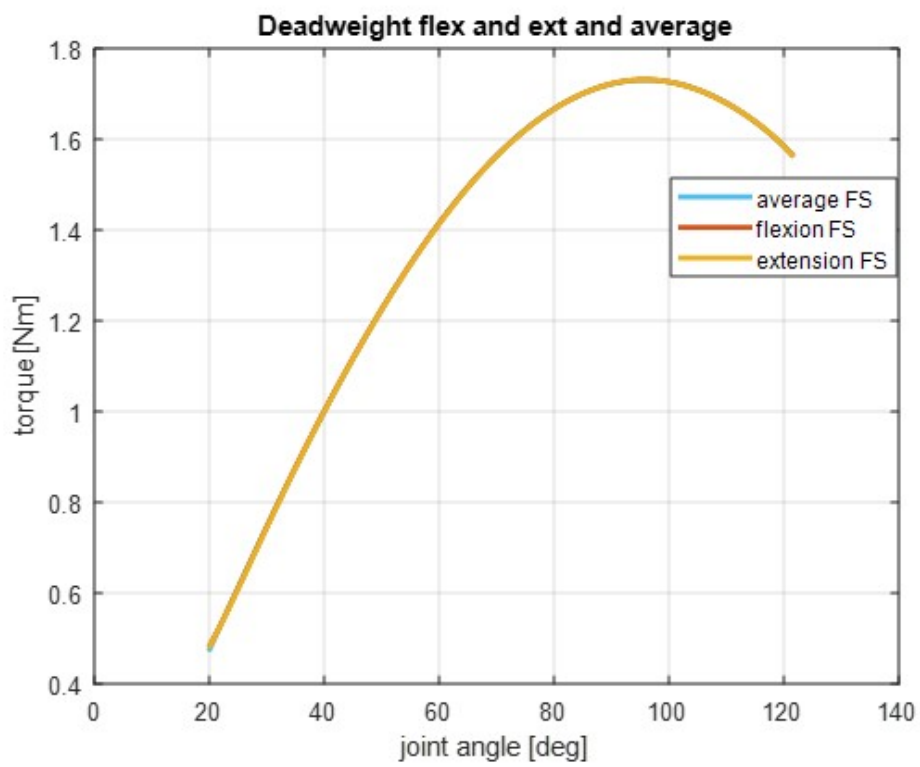


Figure 7.6: After interpolation, the mean among the cycles for each direction and measuring source are calculated.

7.1.5 Stats calculation

The root mean square error between model/adaptive model and measured data calculated:

$$RMSE = \sqrt{\frac{\sum_{n=1}^n (T_{model_n} - T_{measure_n})^2}{n}}$$

In addition, the coefficient of determination (also called R square) between model/adaptive model and measured result are calculated:

$$R^2 = 1 - \frac{\sum_{n=1}^n (T_{measure_n} - T_{model_n})^2}{\sum_{n=1}^n (T_{measure_n} - T_{measure_mean})^2}$$

7.2 Initial measurement and Parameter estimation of the human experiment

This section describes how the initial measurements was taken before the experiment and how the parameter estimation was calculated from those measurements. Since unlike dead weight experiment, two model parameters: Forearm Mass and center of mass could not be measured directly, but only through approximation: The mass and center of mass of the forearm and hand.

7.2.1 Initial measurement

First, Each participant was asked to answer information about its basic profile: Height, Age, Body weight, Sport frequency, Dominant arm.

Moreover, the participant was asked to stand straight and kept its arm at a neutral comfortable position, then the length of forearm and forearm with hand were measured. We followed the measured protocol described by Winter (2009) : The forearm is the distance between "elbow axis to ulnar styloid"; The forearm with hand is the distance between "elbow axis to second knuckle middle finger" (Winter, 2009).

Last, the participant was asked to stand in front of a cylinder-shaped water bucket and immersed its forearm into a cylinder water tank, the subject stopped when its ulnar styloid was immersed to record change of water level, this measured the hand volume. Afterwards, the participant fully immersed

CHAPTER 7. APPENDIX

its forearm up to the level of its elbow axis, this measured the volume of forearm with hand.

7.2.2 Mass estimation

From initial measurement, the forearm volume was calculated by change of water level in the tank with 0.0082 m^2 bottom area :

$$Volume_{Forearm} = 0.082 * \Delta$$

$$Volume_{Hand} = 0.082 * \Delta$$

$$Volume_{Forearmwithhand} = 0.082 * \Delta$$

Δ represents changes of water level. The mass of the forearm was estimated by multiplying the volume of the forearm and used an assumed density of the forearm (1.09 kg/L); 1.12 kg/L for hand only and 1.14 kg/L for Forearm with hand from the bio metric table (Winter, 2009):

$$Mass_{Forearm} = 1.09 * Volume_{Forearm}$$

$$Mass_{hand} = 1.12 * Volume_{Hand}$$

$$Mass_{foreamwithhand} = 1.14 * Volume_{Forearmandhand}$$

7.2.3 Center of mass estimation

The center of mass was estimated from proportion of segment length measurements: From the proximal direction, the center of mass of the forearm is located at 0.506 for hand and 0.403 for forearm. By knowing individual center of mass from hand and forearm segment, hence the shared center of mass with forearm and hand is:

$$X_{forearmwithhand} = \frac{Mass_{Forearm} * 0.403 * L_{Forearm} + Mass_{Hand} * (0.506 * L_{hand} + L_{forearm})}{Mass_{Forearm} + Mass_{Hand}}$$

7.3 Human data process

The force data from human has similar procedure us the dead weight experiment. There is one discrepancy: Additional step to exclude data based on EMG activity and video record, note that this process only applies on dynamic measurement only since it has multiple samples to start with. The whole processing diagram is shown in (Fig 7.7).

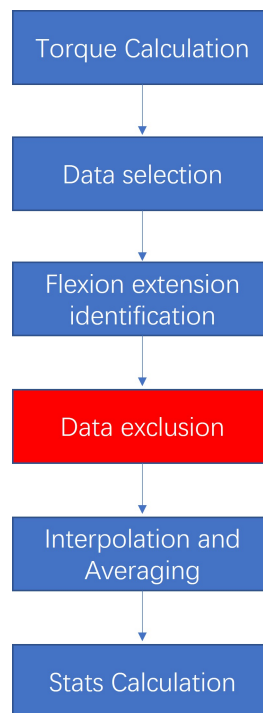


Figure 7.7: The work flow of processing joint torque subject data in this experiment. It's similar to the dead weight data procedure, but requires additional step on data exclusion (marked in red block).

7.3.1 Data exclusion

Data from human dynamic experiment are excluded under three exclusion criteria: Start and end exclusion, EMG exclusion and video record exclusion.

For each measurement, the first and the last cycle are excluded (Cycle 1 and Cycle 8) since these data are the starting and ending point of the measurement which might have abnormal measurements when measurement initiates or ends.

During the measurement, the participant was required to keep its arm slack for whole measurement in order to measure passive force accurately. This exclusion is evaluated by synchronized ENG data. A upper threshold was calculated based on the result from participant relaxed EMG measurement:

$$Threshold = EMG_{mean} + 3 * EMG_{std}$$

For each flex/ext cycle from each sensor, it detects percentage of data exceeds the threshold, once a sensor cycle exceed 5% is considered generating voluntary force thus the corresponding force data is excluded, one example in between plot of EMG is illustrated in (Fig 7.8), this part of the code was written by Kyriacos Papa.

Furthermore, from video record, force data is excluded if participant was found to have behaviors that effect force measurement like moving its arm, moving its body, turning its head, touch objects, etc. One of the example is illustrated in (Fig 7.9).

7.4 Data exclusion on Subject 03 and Subject 10

After data processing, all the averaged joint torque is reinterpolated under same data size and plotted together in a group plot, as illustrated in (Fig 7.10). Subject 03 data is substantially higher than the value of other measurements in both static and dynamic measurements.

After subtracting the presumed impedance by utilizing data from 90 deg abduction measurement, the torque vs joint angle can be seen in Fig 7.11. Beside Subject 03, value of Subject 10 is also exhibits different shape among other measurements in both static and dynamic measurements, even though it does not exhibit as an outlier before joint impedance subtraction, this suggests that its 90 deg measurements are substantially different among other measurements.

Overall, it's obvious that the measurement from Subject 03 and Subject 10 are outlier as its shape or magnitude is substantially different among others,

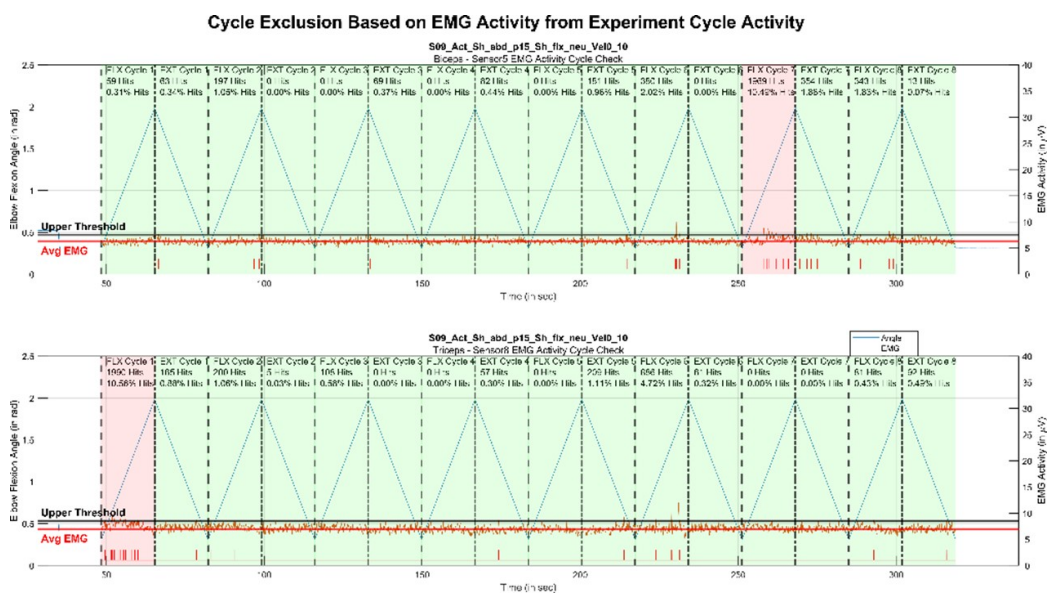
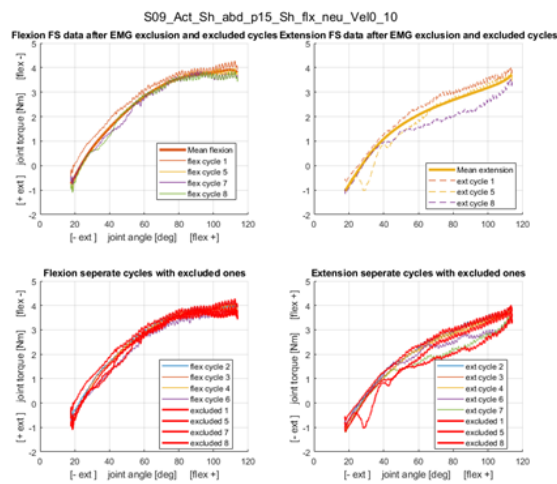


Figure 7.8: In this example from Subject 09, cycle 7 flexion is excluded based on sensor 5 measurement. In addition, cycle 1 flexion also exceeds threshold in sensor 8 measurement but it is already being excluded automatically due to auto exclusion rule of cycle 1 and cycle 8. Excluded cycles are marked in red while the rest are marked in green.

CHAPTER 7. APPENDIX



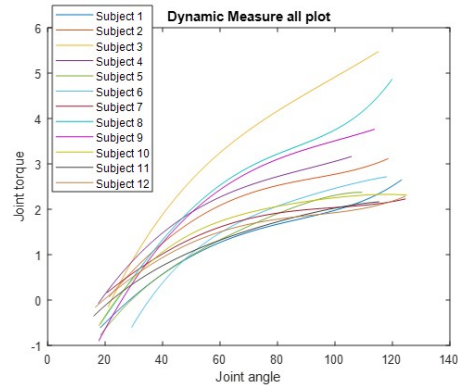
(a) Participant finger touches obstacle at cycle 05 extension.



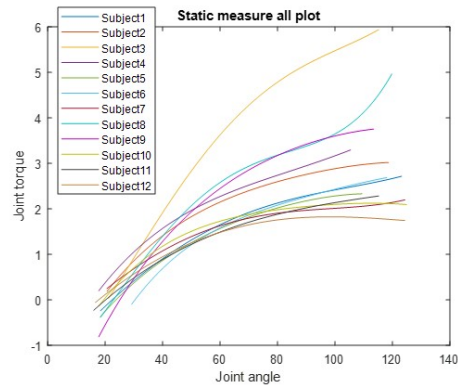
(b) In-between plot shows that the cycle is excluded.

Figure 7.9: Since the participant Subject 09 finger touched the obstacle on extension cycle 05, this cycle is excluded. Cycle 07 flx was excluded due to EMG activity as mentioned in (Fig 7.8).

thus the conclusion is to exclude these two data in further calculation.



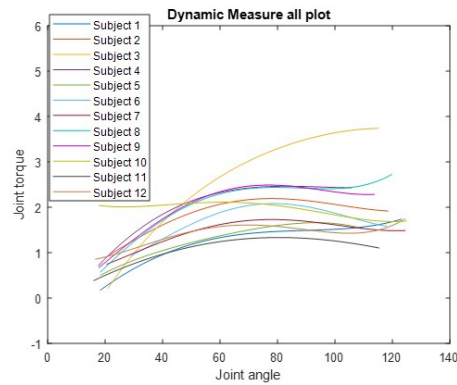
(a) Averaged Dynamic measurement vs Joint angle



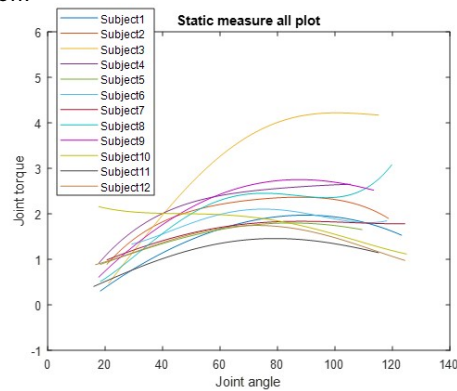
(b) Averaged Static measurement vs Joint angle

Figure 7.10: Subject 03 data is substantially higher than the value of others from both dynamic and static measurements.

CHAPTER 7. APPENDIX



(a) Averaged Dynamic measurement vs Joint angle after joint impedance subtraction.



(b) Averaged Static measurement vs Joint angle after joint impedance subtraction.

Figure 7.11: Subject 03 data is substantially higher than the value of others from both dynamic and static measurements. Subject 10 data value is also different from other measurements after joint impedance subtraction.

CHAPTER 7. APPENDIX

Bibliography

- Angelini, C. and Tasca, E. (2012). Fatigue in muscular dystrophies. *Neuromuscul Disord*, 22 Suppl 3(3-3):S214–20.
- Arakelian, V. (2015). Gravity compensation in robotics. *Advanced Robotics*, 30:1–18.
- Bushby, K., Finkel, R., Birnkrant, D. J., Case, L. E., Clemens, P. R., Cripe, L., Kaul, A., Kinnett, K., McDonald, C., Pandya, S., Poysky, J., Shapiro, F., Tomezsko, J., and Constantin, C. (2010a). Diagnosis and management of duchenne muscular dystrophy, part 1: diagnosis, and pharmacological and psychosocial management. *Lancet Neurol*, 9(1):77–93.
- Bushby, K., Finkel, R., Birnkrant, D. J., Case, L. E., Clemens, P. R., Cripe, L., Kaul, A., Kinnett, K., McDonald, C., Pandya, S., Poysky, J., Shapiro, F., Tomezsko, J., and Constantin, C. (2010b). Diagnosis and management of duchenne muscular dystrophy, part 2: implementation of multidisciplinary care. *Lancet Neurol*, 9(2):177–89.
- Ellis, J. A., Vroom, E., and Muntoni, F. (2013). 195th enmc international workshop: Newborn screening for duchenne muscular dystrophy 14–16th december, 2012, naarden, the netherlands. *Neuromuscular Disorders*, 23(8):682–689.
- Estilow, T., Glanzman, A., Flickinger, J., Powers, K. M., Moll, A., Medne, L., Tennekoon, G., and Yum, S. W. (2014). G.p.99: The wilmington robotic exoskeleton (wrex) improves upper extremity function in patients with duchenne muscular dystrophy. *Neuromuscular Disorders*, 24(9):824–825.
- Guidali, M., Keller, U., Klamroth-Marganska, V., Nef, T., and Riener, R. (2013). Estimating the patient’s contribution during robot-assisted therapy. *Journal of Rehabilitation Research and Development*, 50(3):379–394.

BIBLIOGRAPHY

- He, J., Koeneman, E. J., Schultz, R. S., Herring, D. E., Wanberg, J., Huang, H., Sugar, T., Herman, R., and Koeneman, J. B. (2005). Rupert: a device for robotic upper extremity repetitive therapy. *Conference proceedings : ... Annual International Conference of the IEEE Engineering in Medicine and Biology Society. IEEE Engineering in Medicine and Biology Society. Conference*, 7:6844–7.
- Janssen, M., Harlaar, J., Koopman, B., and de Groot, I. J. M. (2017). Dynamic arm study: quantitative description of upper extremity function and activity of boys and men with duchenne muscular dystrophy. *J Neuroeng Rehabil*, 14(1):45.
- Just, F., Özen, z., Tortora, S., Klamroth-Marganska, V., Riener, R., and Rauter, G. (2020). Human arm weight compensation in rehabilitation robotics: efficacy of three distinct methods. *Journal of NeuroEngineering and Rehabilitation*, 17.
- Kearney, R. E. and Hunter, I. W. (1990). System identification of human joint dynamics. *Critical reviews in biomedical engineering*, 18(1):55–87.
- Kooren, P. N., Lobo-Prat, J., Keemink, A. Q. L., Janssen, M. M., Stienen, A. H. A., De Groot, I. J. M., Paalman, M. I., Verdaasdonk, R., and Koopman, B. F. J. M. (2016). Design and control of the active a-gear: A wearable 5 dof arm exoskeleton for adults with duchenne muscular dystrophy. In *Proceedings of the IEEE RAS and EMBS International Conference on Biomedical Robotics and Biomechanics*, volume 2016-July, pages 637–642.
- Kumar, A. and Phillips, M. F. (2013). Use of powered mobile arm supports by people with neuromuscular conditions. *J Rehabil Res Dev*, 50(1):61–70.
- Landfeldt, E., Mayhew, A., Eagle, M., Lindgren, P., Bell, C. F., Guglieri, M., Straub, V., Lochmüller, H., and Bushby, K. (2015). Development and psychometric analysis of the duchenne muscular dystrophy functional ability self-assessment tool (dmdsat). *Neuromuscul Disord*, 25(12):937–44.
- Liu, S., Wang, Y., Xie, Y., Jiang, S., and Meng, J. (2009). A new cerebellar model articulation controller for rehabilitation robots. In *Lecture Notes in Computer Science (including subseries Lecture Notes in Artificial Intelligence and Lecture Notes in Bioinformatics)*, volume 5553 LNCS, pages 207–216.
- Lobo-Prat, J., Keemink, A. Q. L., Koopman, B. F. J. M., Stienen, A. H. A., and Veltink, P. H. (2016a). Adaptive gravity and joint stiffness

BIBLIOGRAPHY

- compensation methods for force-controlled arm supports. In *IEEE International Conference on Rehabilitation Robotics*, volume 2015-September, pages 478–483.
- Lobo-Prat, J., Kooren, P. N., Janssen, M. M. H. P., Keemink, A. Q. L., Veltink, P. H., Stienen, A. H. A., and Koopman, B. F. J. M. (2016b). Implementation of emg-and force-based control interfaces in active elbow supports for men with duchenne muscular dystrophy: a feasibility study. *IEEE Transactions on Neural Systems and Rehabilitation Engineering*, 24(11):1179–1190.
- Lobo-Prat, J., Kooren, P. N., Keemink, A. Q. L., Paalman, M. I., Hekman, E. E. G., Veltink, P. H., Stienen, A. H. A., and Koopman, B. F. J. M. (2014). Design and control of an experimental active elbow support for adult duchenne muscular dystrophy patients. In *Proceedings of the IEEE RAS and EMBS International Conference on Biomedical Robotics and Biomechatronics*, pages 187–192.
- McPherson, A., Matthew, R., Estrada, M., Bajcsy, R., and Tomizuka, M. (2020). Design of a passive, variable stiffness exoskeleton for triceps deficiency mitigation. *Annu Int Conf IEEE Eng Med Biol Soc*, 2020:4921–4925.
- Mercuri, E., Bönnemann, C. G., and Muntoni, F. (2019). Muscular dystrophies. *Lancet*, 394(10213):2025–2038.
- Oliveira, A. C. d., Warburton, K., Sulzer, J. S., and Deshpande, A. D. (2019). Effort estimation in robot-aided training with a neural network. In *2019 International Conference on Robotics and Automation (ICRA)*, pages 563–569.
- Rahman, T., Ramanathan, R., Stroud, S., Sample, W., Seliktar, R., Harwin, W., Alexander, M., and Scavina, M. (2001). Towards the control of a powered orthosis for people with muscular dystrophy. *Proceedings of the Institution of Mechanical Engineers, Part H: Journal of Engineering in Medicine*, 215(3):267–274.
- Rosen, J., Perry, J., Manning, N., Burns, S., and Hannaford, B. (2005). *The human arm kinematics and dynamics during daily activities - toward a 7 DOF upper limb powered exoskeleton*, volume 2005.
- Spong, M. W., Hutchinson, S., and Vidyasagar, M. (2006). *Robot modeling and control*. John Wiley & Sons, Hoboken, NJ.

BIBLIOGRAPHY

- Winter, D. A. (2009). *Biomechanics and motor control of human movement*. John Wiley & Sons.
- Xie, Q. L., Meng, Q. L., Zeng, Q. X., Fan, Y. J., Dai, Y., and Yu, H. L. (2021). Human-exoskeleton coupling dynamics of a multi-mode therapeutic exoskeleton for upper limb rehabilitation training. *IEEE ACCESS*, 9:61998–62007.